

**FULL PAPER**

# Novel 1,2,4-triazole derivatives: Design, synthesis, anticancer evaluation, molecular docking, and pharmacokinetic profiling studies

Abdallah Turkey<sup>1</sup> | Farag F. Sherbiny<sup>1,2</sup> | Ashraf H. Bayoumi<sup>1</sup> | Hany E. A. Ahmed<sup>1,3</sup> | Hamada S. Abulkhair<sup>1,4</sup> 

<sup>1</sup>Pharmaceutical Organic Chemistry Department, Faculty of Pharmacy, Al-Azhar University, Nasr City, Cairo, Egypt

<sup>2</sup>Pharmaceutical Organic Chemistry Department, College of Pharmacy, Misr University for Science and Technology (MUST), 6th October City, Egypt

<sup>3</sup>Pharmacognosy and Pharmaceutical Chemistry Department, Pharmacy College, Taibah University, Al-Madinah, Al-Munawarah, Saudi Arabia

<sup>4</sup>Pharmaceutical Chemistry Department, Faculty of Pharmacy, Horus University, New Damietta, Egypt

**Correspondence**

Hamada S. Abulkhair, Pharmaceutical Organic Chemistry Department, Faculty of Pharmacy, Al-Azhar University, Nasr City, Cairo 11884, Egypt.

Email: [hamadaorganic@azhar.edu.eg](mailto:hamadaorganic@azhar.edu.eg)

**Abstract**

Three novel series of 1,2,4-triazole derivatives were designed and synthesized as potential adenosine A2B receptor antagonists. The design of the new compounds depended on a virtual screening of a previously constructed library of compounds targeting the human adenosine A2B protein. Spectroscopic techniques including <sup>1</sup>H nuclear magnetic resonance (NMR) and <sup>13</sup>C NMR, and infrared and mass spectroscopy were used to confirm the structures of the synthesized compounds. The in vitro cytotoxicity evaluation was carried out against a human breast adenocarcinoma cell line (MDA-MB-231) using the MTT assay, and the obtained results were compared with doxorubicin as a reference anticancer agent. In addition, in silico studies to propose how the two most active compounds interact with the adenosine A2B receptor as a potential target were performed. Furthermore, a structure–activity relationship analysis was performed, and the pharmacokinetic profile to predict the oral bioavailability and other pharmacokinetic properties was also explained. Four of our designed derivatives showed promising cytotoxic effects against the selected cancer cell line. Compound **15** showed the highest activity with an IC<sub>50</sub> value of 3.48 μM. Also, compound **20** revealed an equipotent activity with the reference cytotoxic drug, with an IC<sub>50</sub> value of 5.95 μM. The observed IC<sub>50</sub> values were consistent with the obtained in silico docking scores. The newly designed compounds revealed promising pharmacokinetic profiles as compared with the reference marketed drug.

**KEYWORDS**

A2B receptor antagonist, anticancer, molecular docking, triazoles

## 1 | INTRODUCTION

Extracellular adenosine is a nucleoside that regulates cell function via binding to specific receptors on its surface.<sup>[1]</sup> The two main sources of extracellular adenosine are the exocytosis of intracellular adenosine and the enzymatic breakdown of extracellular adenosine triphosphate (ATP).<sup>[2]</sup> Besides its importance in the production of ATP, adenosine mediates various pharmacological effects, both in the peripheral and in the central nervous system (CNS).<sup>[3]</sup> Under cellular stress, the elevation

of intracellular adenosine levels triggers a concomitant active transport of adenosine into the extracellular space and subsequent activation of different adenosine receptors.<sup>[4]</sup> To date, four subtypes of adenosine receptors, termed A1, A2A, A2B, and A3, have been determined. Each subtype of adenosine receptors has its unique pharmacological profile.<sup>[5]</sup> Unlike A1, A2A, and A3 adenosine receptors, the A2B subtype binds with a lower affinity to adenosine. So, a high level of adenosine is required for the activation of A2B.<sup>[6]</sup> Thus, stimulation of A2B receptors participates in several pathophysiological disorders as in the case of tumors and

ischemia.<sup>[7,8]</sup> In addition, the adenosine A2B receptors are highly expressed in the microvascular endothelial cells, where they regulate the angiogenic factors and subsequently angiogenesis, which is one of the major approaches for regulation and control of tumor growth.<sup>[9]</sup> Therefore, the management of cancer is one of the therapeutic profiles of the adenosine A2B receptor subtype.<sup>[10]</sup>

A piece of evidence for the overexpression of A2B adenosine receptors in the human breast adenocarcinoma (MDA-MB-231)<sup>[7,11,12]</sup> has been proved. Consequently, a virtual screening of potential A2B antagonistic ligands using the adenosine A2B receptor homology model has been performed,<sup>[13]</sup> which led to the identification of a library of antagonistic candidates for the adenosine A2B receptors. However, potential hits suggested in this study need further experimental analysis to confirm the results. Out of the 250 identified novel candidates, 20 ligands belong to the 3,4,5-trisubstituted-1,2,4-triazole scaffold. All are attached with two aryl moieties at both N-4 and C-5, together with a hydrophilic linker in the form of either an *N*-(aryl)acetamide or *N*-(aryl)propanamide at C-3. One of the most potent and potentially selective hits in this study is the 2-[[4-(3-chloro-2-methylphenyl)-5-(pyridin-4-yl)-4*H*-1,2,4-triazol-3-yl]thio]-*N*-(3-methoxyphenyl)acetamide (**1**). Additionally, 1,2,4-triazoles have emerged in the last decade as therapeutic drugs due to their diverse biological activities, particularly as an antiproliferative agent.<sup>[14,15]</sup> The 1,2,4-triazole ring has the advantage of providing good water solubility, and the potential to interact with a number of enzymes included in cancer gross through its ability to form hydrogen bonds with receptors.<sup>[16]</sup> Compounds **2** and **3** (Figure 1) proved as a potent cytotoxic agent against HCT116 and HepG2 cell lines with low IC<sub>50</sub> values.<sup>[17,18]</sup> Furthermore, a number of 1,2,4-triazole incorporating derivatives have been reported recently as A2B receptor antagonists.<sup>[19–21]</sup>

Furthermore, the *S*-alkylated mercapto-1,2,4-triazoles attached at C-3 with hydrogen bond donor/acceptor atoms, like compounds 4–7 (Figure 2), were reported to exhibit a significant anticancer activity against a panel of cancer cell lines.<sup>[22]</sup> Moreover, a lot of compounds containing *N*-arylacetamide and/or phenacyl moieties have been reported as potent cytotoxic agents.<sup>[23–26]</sup>

## 1.1 | Rationale and structure-based design

Pharmacophoric groups presented in the core structure of the above-mentioned hit (compound **1**) include a heterocyclic nucleus attached directly with aryl rings at N-4 and C-5, as well as a hydrophilic spacer

followed by a lipophilic tail at C-3. Compound **1** consists of a 1,2,4-triazole ring system attached with phenyl and pyridyl substituents at N-4 and C-5, respectively. Also, there is a hydrophilic linker in the form of an *N*-arylacetamide moiety at C-3, followed by a lipophilic tail. The proposed binding mode of compound **1** with the active site of A2B receptor involves three main interactions. The N-1 of triazole and the pyridyl nitrogen are involved in hydrogen bonding interactions with Asn254 and Thr89 residues, respectively. The pyridyl ring at C-5 showed  $\pi$ - $\pi$  stacking with His280 and Ser279. The terminal *N*-aryl moiety occupied the hydrophobic bucket composed of Val253 and Met179 amino acid residues (Figure 3). Owing to these desirable interactions, compound **1** showed a good affinity toward the human adenosine A2B receptor.

In light of the aforementioned facts and as a continuation of our previous studies on identification of new anticancer agents,<sup>[21,27–29]</sup> the main objective of the present work is to design and synthesize a new set of 1,2,4-triazole derivatives with the same structural features of the hit compound **1** and almost the same binding mode with the A2B receptor. Herein, inspired by the versatility of the 1,2,4-triazole ring, three novel series of analogous structures were designed and synthesized (Figure 4) to evaluate their anticancer activity. Only three bioisosteric modifications were achieved in the designed new triazole derivatives: (a) replacement of the pyridyl group at C-5 with the isosteric phenyl ring, which is either unsubstituted or attached with an electron-donating group at the *para* position; (b) replacement of the methoxyphenyl attached to the terminal hydrophilic tail with either monosubstituted phenyl or naphthyl ring system; (c) replacement of the hydrophilic linker at C-3 with another one in which both the length and number of hydrogen bond donors/acceptors decreased. Different substitution patterns were incorporated into phenyl groups at both C-5 of the triazole ring and the terminal hydrophilic tail to investigate the effect of these structural modifications on the cytotoxicity of the designed compounds. This variety of structural modifications enabled us to examine the structure–activity relationship (SAR) of the new derivatives as potential anticancer agents. All the synthesized compounds were evaluated for their *in vitro* cytotoxic activity against the human breast adenocarcinoma (MDA-MB-231) cells as a proposed model for the A2B adenosine receptor subtype.<sup>[7]</sup>

## 2 | RESULTS AND DISCUSSION

### 2.1 | Chemistry

In the present study, final target compounds of the 1,2,4-triazole scaffold were achieved in four consecutive steps, utilizing

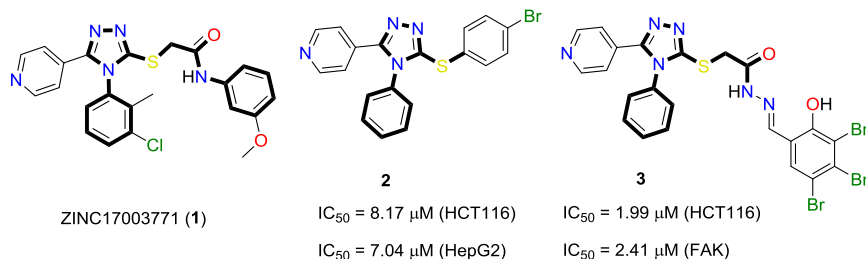


**FIGURE 1** Reported lead 1,2,4-triazole derivative as a potent A2B antagonist and structures of selected potent 1,2,4-triazole anticancer agents

**FIGURE 2** The S-alkylated mercapto-1,2,4-triazoles attached with hydrogen bond donor/acceptor as potential anticancer agents

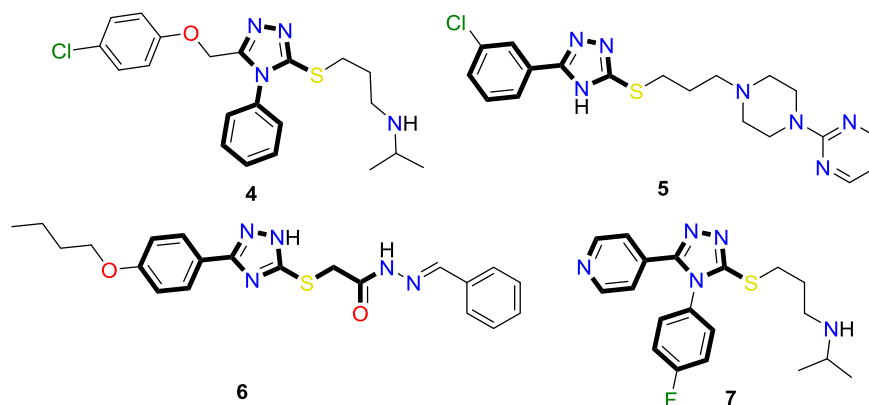
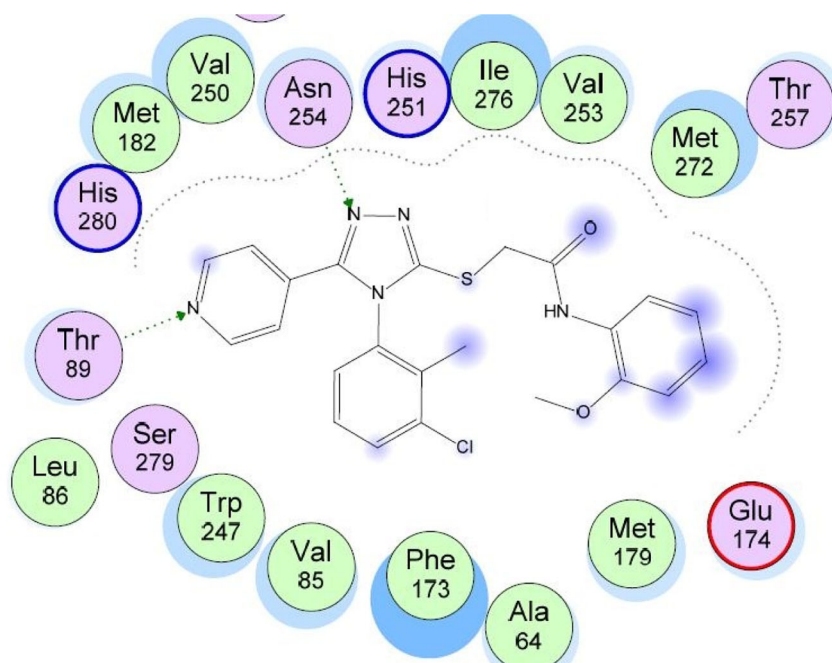


**FIGURE 3** The predicted binding mode for compound 1 with the homology model of the human adenosine A2B receptor



commercially available unsubstituted or *para*-substituted benzoic acid. The general route for the synthesis of the designed 1,2,4-triazole derivatives is illustrated in Scheme 1. The appropriate acid was converted to the corresponding ester by the action of absolute

ethanol in the presence of a catalytic amount of concentrated sulfuric acid. The produced esters were treated with hydrazine hydrate in ethanol<sup>[30]</sup> to yield the hydrazide derivatives **10a–c**. The latter reacted under reflux with phenyl isothiocyanate<sup>[22,31]</sup> in an alcoholic

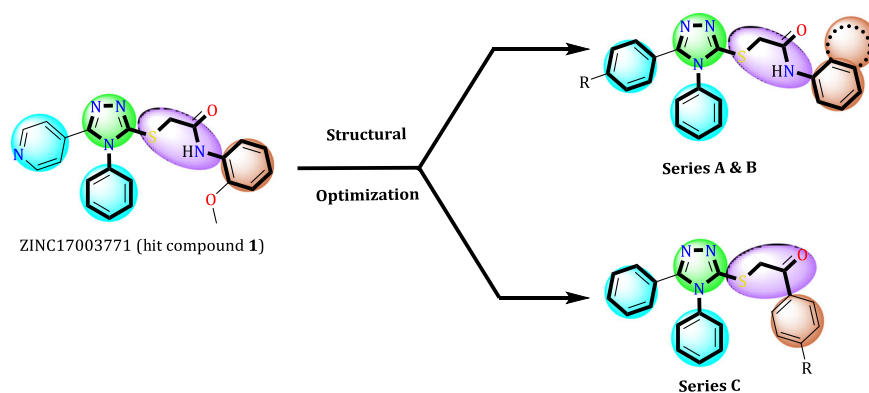
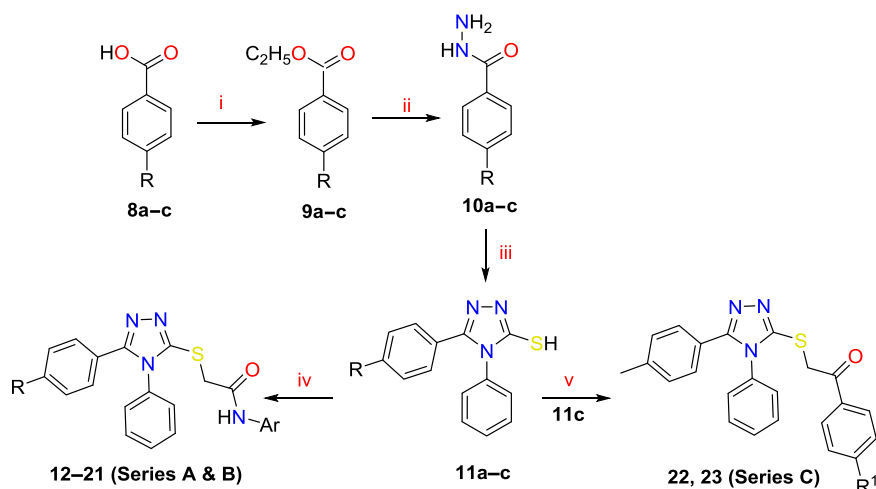


**FIGURE 4** The hit compound and structure-based design of the newly designed derivatives



**SCHEME 1** The synthetic route of the designed new 1,2,4-triazole derivatives

#### Reagents and conditions:

- i)** C<sub>2</sub>H<sub>5</sub>OH/Conc H<sub>2</sub>SO<sub>4</sub>, 120°C, 70–77%; **ii)** H<sub>2</sub>N-NH<sub>2</sub>·H<sub>2</sub>O, C<sub>2</sub>H<sub>5</sub>OH, 100°C, 80–84%.  
**iii)** 1- C<sub>6</sub>H<sub>5</sub>NCS/KOH, 2- HCl, 120°C 67–78%; **iv)** ClCH<sub>2</sub>CONHAr/(C<sub>2</sub>H<sub>5</sub>)<sub>3</sub>N, 90°C, 70–85%.  
**v)** ClCH<sub>2</sub>COAr/(C<sub>2</sub>H<sub>5</sub>)<sub>3</sub>N, 90°C, 84–89%;

#### Series A, R = H

- 12:** Ar = 4-BrC<sub>6</sub>H<sub>4</sub>  
**13:** Ar = 4-ClC<sub>6</sub>H<sub>4</sub>  
**14:** Ar = 4-CH<sub>3</sub>C<sub>6</sub>H<sub>4</sub>  
**15:** Ar = 4-OCH<sub>3</sub>C<sub>6</sub>H<sub>4</sub>  
**16:** Ar = 1-Naphthyl

#### Series B, R = Cl

- 17:** Ar = 4-BrC<sub>6</sub>H<sub>4</sub>  
**18:** Ar = 4-ClC<sub>6</sub>H<sub>4</sub>  
**19:** Ar = 4-CH<sub>3</sub>C<sub>6</sub>H<sub>4</sub>  
**20:** Ar = 4-OCH<sub>3</sub>C<sub>6</sub>H<sub>4</sub>  
**21:** Ar = 1-Naphthyl

#### Series C

- 22:** R<sup>1</sup> = CH<sub>3</sub>  
**23:** R<sup>1</sup> = Cl

solution of KOH to yield the potassium salts of 4-phenyl-5-(aryl)-4H-1,2,4-triazole-3-thiol (**11a-c**), which readily converted into the parent thioalcohol by the action of hydrochloric acid. Compounds **11a,b** were finally treated with the appropriate previously prepared 2-chloro-N-arylacetylacetamide derivatives<sup>[32]</sup> in the presence of potassium hydroxide to produce target compounds **12-21** in relatively good yields and reasonable purities. Alternatively, treating **11c** with the appropriate 2-bromo-1-arylethan-1-one derivative in the presence of potassium hydroxide afforded target compounds **22** and **23**.

Structures and purities of this new set of 2-[(4,5-diaryl-4H-1,2,4-triazol-3-yl)thio]-N-arylacetylacetamide derivatives were confirmed on the basis of spectral data and thin-layer chromatography (TLC). In all compounds, infrared (IR) spectra showed stretching bands between 3,416 and 3,452 cm<sup>-1</sup>, which represent the secondary amide NH functionality. In addition, typical amide carbonyl stretching bands between 1,670 and 1,682 cm<sup>-1</sup> were observed in all spectra. Collectively, these observations with the disappearance of the SH signals in <sup>1</sup>H nuclear magnetic resonance (NMR) spectra of compounds **11a,c** confirm tethering of the acetamide or ketone moiety with triazole nucleus in the final compounds via S-linkage. The NH groups revealed singlet signals, which are D<sub>2</sub>O-exchangeable, equivalent to one proton, around 10.40 ppm. Aliphatic (S-CH<sub>2</sub>) protons revealed singlet signals around 4.16 ppm. Mass spectra of all compounds are

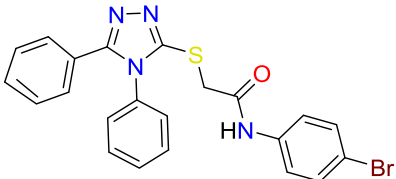
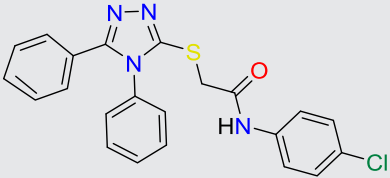
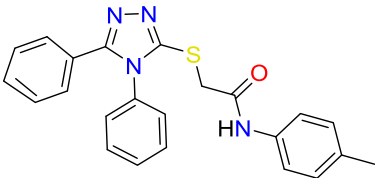
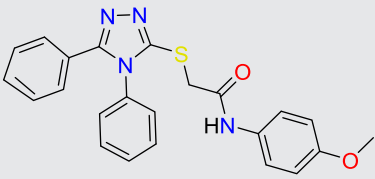
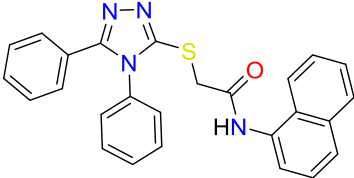
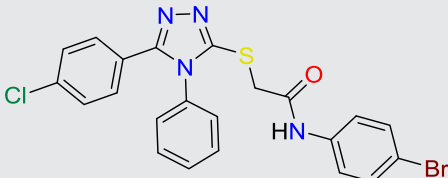
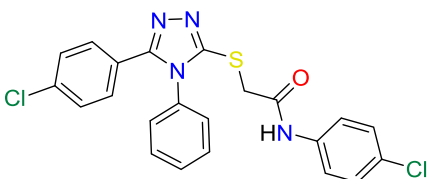
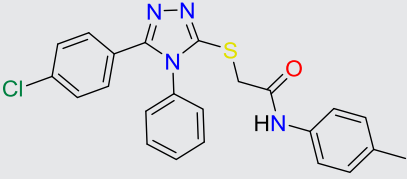
characterized by the presence of distinctive molecular ion peaks at the expected *m/z* values.

## 2.2 | Evaluation of biological activity

### 2.2.1 | Cytotoxicity assay

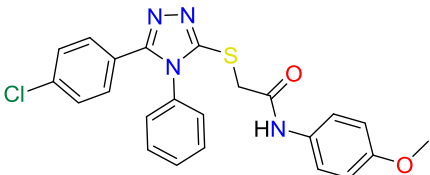
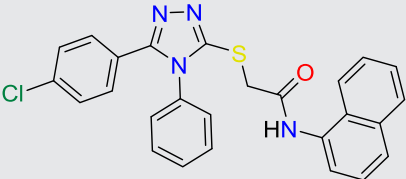
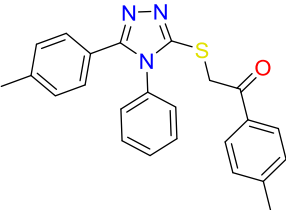
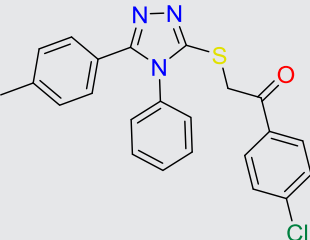
The cytotoxic activity of the newly synthesized compounds was evaluated against human breast adenocarcinoma cancer cells (MDA-MB-231) using the MTT (3-(4,5-dimethylthiazol-2-yl)-2,5-diphenyltetrazolium bromide) assay,<sup>[33]</sup> and doxorubicin was used as a reference anticancer agent. Results of the preliminary antiproliferative evaluation are shown in Table 1. Most of the synthesized compounds displayed mild-to-moderate cytotoxic activity. Concentrations of target compounds needed to inhibit 50% of tumor cell proliferation were as low as 3.48 μM. Compounds **13**, **15**, **19**, and **20** were the most potent derivatives. Compound **15** showed a more powerful inhibitory effect than doxorubicin, with an IC<sub>50</sub> value of 3.48 μM. Also, compound **20** revealed an equipotent activity with the reference cytotoxic drug against the selected cancer cell line. Higher doses (up to 17.37 μM) of derivatives **13** and **19** were needed to inhibit 50% of cell proliferation, indicating moderate activity of these two derivatives.

**TABLE 1** In vitro anticancer activity of the designed 1,2,4-triazoles against the human breast adenocarcinoma (MDA-MB-231) cancer cell line

Compound	Chemical structure	IC <sub>50</sub> (μM) <sup>a</sup>
12		32.73 ± 0.88
13		17.37 ± 1.01
14		>100
15		3.48 ± 0.34
16		57.50 ± 0.86
17		30.90 ± 0.88
18		27.50 ± 0.68
19		10.96 ± 0.74

(Continues)

TABLE 1 (Continued)

Compound	Chemical structure	IC <sub>50</sub> (μM) <sup>a</sup>
20		5.95 ± 0.97
21		>100
22		39.53 ± 0.96
23		>100
Doxorubicin		4.50 ± 0.27

Note: Data here are presented as the means of five independent experiments ± standard deviation.

<sup>a</sup>Cytotoxicity was assayed by treating cells with the test compound for 72 hr and expressed as the concentration needed to inhibit 50% of tumor cell proliferation (IC<sub>50</sub>).

## 2.2.2 | SAR study

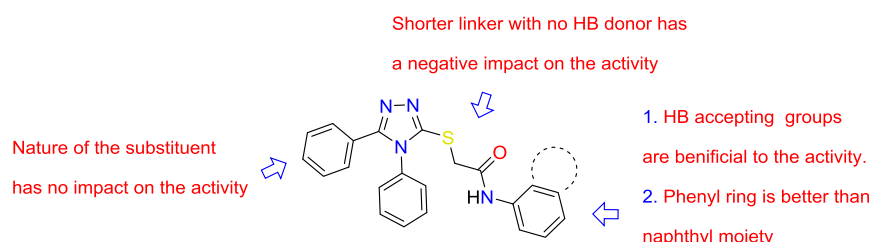
As outlined in the rationale structure-based drug design, investigation of SAR of newly synthesized compounds as cytotoxic agents is a major objective of the present work. Results of cytotoxicity evaluation could be summarized as follows: (a) Ketone derivatives of series C exhibited a lower activity, compared with the acetamide derivatives of series A and B, which reflects the importance of NH in the hydrophilic spacer for the activity. (b) The electronic nature of substituents attached to the terminal phenyl ring of hydrophilic tail in series A and B had a considerable influence on the cytotoxic activity. Compounds **12**, **13**, **15**, **18**, and **20** with hydrogen bond acceptor groups attached to C-4 of the terminal phenyl ring displayed remarkable inhibitory effects, with IC<sub>50</sub> values ranging from 3.44 to 32.73 μM. (c) Replacement of the terminal phenyl ring with naphthyl moiety of the same scaffold, as in compounds **16** and **21**, revealed a negative impact on the cytotoxicity (IC<sub>50</sub> values are more than 57 μM). These relatively lower activities of such derivatives may be

attributed to the presence of a bulky group, making these naphthyl derivatives unable to accommodate the size-limited binding pocket of the A2B receptor. Also, replacing the hydrogen bond acceptor attached to the terminal phenyl ring of hydrophilic linker with an alkyl group, as in compounds **14**, resulted in a sharp drop in the antitumor activity, with IC<sub>50</sub> values above 100 μM. Independently, compound **19** showed a moderate activity, with an IC<sub>50</sub> value of 10.96 μM. However, the nature of the substituents attached to the phenyl group at C-5 of the triazole ring had no or little impact on the cytotoxic activity. A summary of the structure-activity relationship of the acetamide derivatives **12–23** is presented in Figure 5.

## 2.3 | Molecular docking studies

In the present work, molecular docking studies were conducted to determine molecular binding modes of target compounds inside the pocket of the adenosine A2B receptor. Docking studies were

**FIGURE 5** A summary of the structure–activity relationship study of the synthesized 1,2,4-triazoles



conducted using AutoDock Vina program to determine the free energy and the virtual binding modes of the new triazoles with the homology model of the human adenosine A2B receptor binding site. Binding free energies of all compounds, together with that of the hit compound, are presented in Table 2. The selection of the most promising molecules depended on the perfect binding mode and the binding free energy.

The triazole ring and amino group of compound 15, as a representative example of triazoles with an HB acceptor at the *para* position of the terminal benzene ring, are involved in a hydrogen bonding interaction with Asn254 and Phe173 residues. Also, the phenyl ring attached to C-5 is anchored by aromatic stacking interactions with Trp247 and His251 residues, and hydrophobic interactions with Leu86, Val85, Val250, and Met182, a pocket that contributes to an increase in the affinity of the compound (Figure 6). In addition, the phenyl ring at the 4-position showed aromatic stacking interactions with His280 and Phe173, and hydrophobic interactions with Ile276, Ile67, Ala64, Ala60, and Ala82. The methoxyphenyl moiety is located in the hydrophobic bucket composed of Val253 and Met179 (Figure 7). The carbonyl moiety is involved in a water-mediated interaction with Lys269. Due to the existence of additional hydrogen bonding and desirable interactions, compounds 15 and 20 presented a higher affinity than other compounds toward the receptor.

The obtained binding mode of compound 20 with the homology model of the human adenosine A2B receptor follows the general

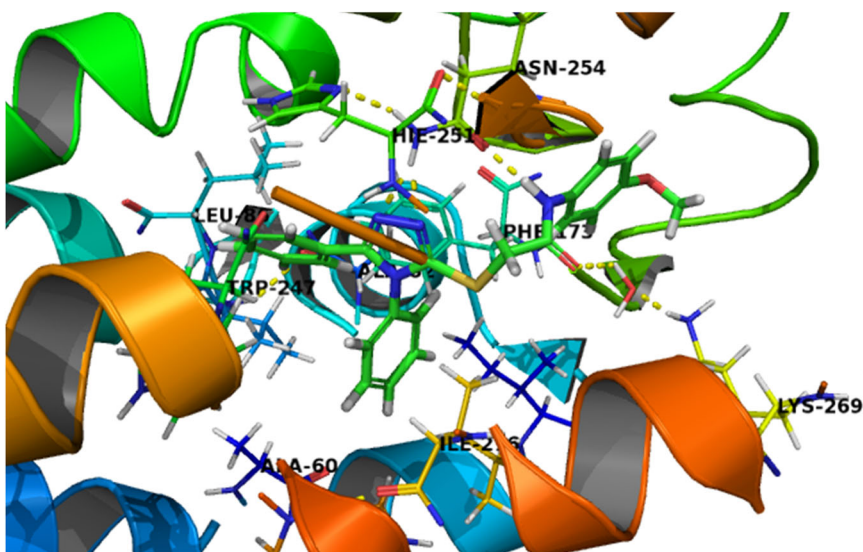
**TABLE 2** The binding free energies ( $\Delta G$ , kcal/mol) of the target new triazoles and the hit compound with the binding site of the human adenosine A2B receptor

Compound	$\Delta G$ (kcal/mol)
1	-11.28
12	-8.12
13	-9.18
14	-7.74
15	<b>-11.17</b>
16	-7.68
17	-8.04
18	-8.75
19	-10.48
20	<b>-10.98</b>
21	-7.83
22	-7.99
23	-7.43

Note: Values made bold for derivatives showing good binding free energy.

pattern observed for compound 15. As before, the hydrogen bonding and aromatic stacking interactions are maintained. The C-5 phenyl ring showed  $\pi$ - $\pi$  stacking with His280 and Phe173, and hydrophobic interactions with Ile276, Ile67, Ala64, Ala60, and Ala82. The terminal

**FIGURE 6** The predicted binding mode for compound 15 with the homology model of the human adenosine A2B receptor. Interactions between H-bonded atoms are indicated by dotted lines. Hydrogen (white), nitrogen (blue), oxygen (red), and sulfur (yellow)



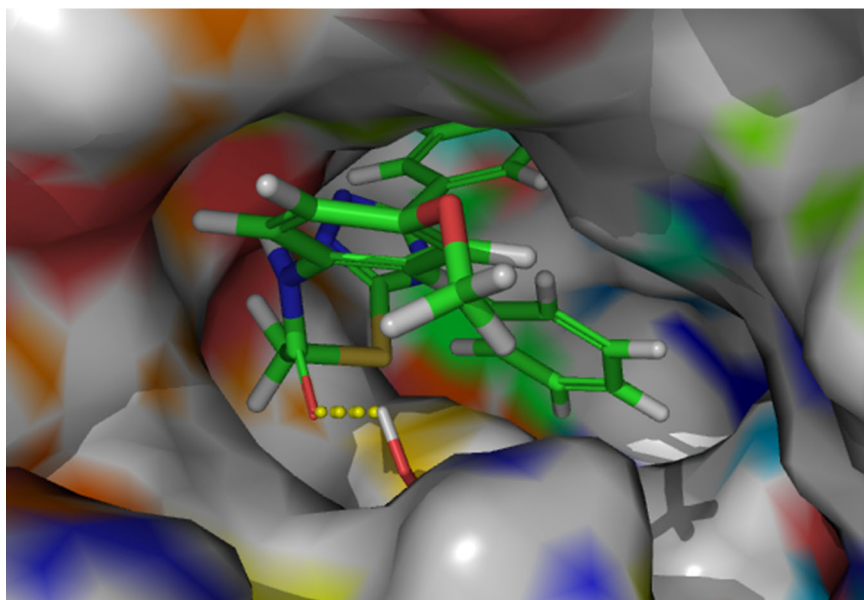


**FIGURE 7** The predicted binding mode for compound **15**, displaying how the compound can accommodate the binding site

methoxyphenyl moiety occupied the hydrophobic bucket composed of Val253 and Met179 amino acid residues. The carbonyl group formed a hydrogen bond with Lys269 residue.

Collectively, the obtained results indicated that all the studied compounds revealed a similar position and orientation inside the putative binding site of the human adenosine A2B receptor. In addition, the results of the binding free energy ( $\Delta G$ ) explain that some of these compounds have a good binding affinity to the receptor and the computed values reflect the overall trend. Furthermore, the present study has highlighted that the triazole moiety is an attractive scaffold for obtaining potent human adenosine A2B receptor. Moreover, the affinity of the ligands would increase if the compounds have the hydrogen bond acceptors on the aromatic substituents where these moieties are located inside the polar groups formed by Asn254, His251, His280, and Glu174. The introduction of a bulky aromatic ring, like naphthalene, decreases the affinity of the compound for the human adenosine A2B receptor.

## 2.4 | Pharmacokinetic profiling study

The pharmacokinetic profile of a compound determines how it would be absorbed, distributed, metabolized, and excreted (ADME). Optimal binding of a new drug with a therapeutic target protein is crucial; however, it is also essential to ensure that it reaches this target in a satisfactory concentration to produce the physiological effect safely. In the present study, absorption, distribution, metabolism, excretion, and toxicity (ADMET) properties of the most active new synthesized compounds were determined using the pkCSM ADMET descriptors algorithm protocol.<sup>[34]</sup> Two main structural features correlate properly with pharmacokinetic properties, the two-dimensional polar surface area (PSA<sub>2D</sub>) and the lipophilicity levels (logP). Absorption of a drug depends on a number of factors, including membrane

permeability (Caco-2), intestinal absorption, skin permeability levels, and P-glycoprotein substrate or inhibitor. Drug distribution depends on the blood–brain barrier (logBB), CNS permeability, and the volume of distribution (VDs). Metabolism is predicted on the basis of the CYP models for substrate or inhibition (CYP2D6, CYP3A4, CYP1A2, CYP2C19, CYP2C9, CYP2D6, and CYP3A4). Excretion is predicted on the basis of the total clearance and the renal OCT2 substrate. The toxicity of the drugs is predicted on the basis of Ames toxicity, hERG inhibition, hepatotoxicity, and skin sensitization. These parameters were calculated for the four most potent cytotoxic compounds, **13**, **15**, **19**, and **20**, as well as for the marketed anticancer drug doxorubicin, and checked for compliance with their standard ranges.

After calculating the ADMET properties (Table 3), we can confirm that the highest potent four triazole derivatives have the advantage of better intestinal absorption in humans, as compared with the reference doxorubicin (91.014, 93.492, 90.909, and 91.928, respectively, compared with 62.372 in case of doxorubicin). This advantage may be attributed to the greater lipophilicity of the designed compounds, which would make it easy to pass through the biological membranes.<sup>[35]</sup> Accordingly, they may have good oral bioavailability in experimental testing. The analysis of the CNS permeability revealed that compounds **13** and **19** have a high ability to penetrate the CNS (CNS permeability values are greater than  $-2.0$ ), whereas doxorubicin is unable to penetrate the CNS (CNS permeability  $< -4.0$ ). These data, unfortunately, indicate that these compounds may present higher side effects in the CNS and lower tolerability among patients.<sup>[35]</sup> It was also possible to observe that in contrast to doxorubicin, compounds **13**, **15**, **19**, and **20** have the potential to inhibit the cytochrome P3A4, the main enzyme accountable for drug metabolism, which is possibly due to the higher lipophilicity of these ligands, thus favoring the inhibition of this CYP enzyme. Excretion was assessed in terms of total clearance. This parameter is related to

**TABLE 3** ADMET profile of the four most active compounds and doxorubicin

Parameter	13	15	19	20	Doxorubicin
<b>Molecular properties</b>					
Molecular weight	420.925	416.502	434.95	450.951	543.525
LogP	5.3185	4.6737	5.62692	5.3271	0.0013
Rotatable bonds	6	7	6	7	5
H-bond acceptors	5	6	5	6	12
H-bond donors	1	1	1	1	6
Surface area	177.297	178.472	183.662	188.776	222.081
<b>Absorption</b>					
Water solubility	-5.034	-4.591	-5.158	-4.738	-2.915
Caco-2 permeability	0.987	1.037	0.98	1.056	0.457
Intestinal absorption (human)	91.014	93.492	90.909	91.928	62.372
Skin permeability	-2.736	93.492	-2.736	-2.736	-2.735
P-glycoprotein substrate	Yes	Yes	Yes	Yes	Yes
P-glycoprotein I inhibitor	Yes	Yes	Yes	Yes	No
P-glycoprotein II inhibitor	Yes	Yes	Yes	Yes	No
<b>Distribution</b>					
VDss (human)	-0.126	-0.235	-0.052	-0.158	1.647
Fraction unbound (human)	0.209	0.23	0.216	0.235	0.215
BBB permeability	0.332	-0.425	0.312	-0.595	-1.379
CNS permeability	-1.832	-2.14	-1.752	-2.02	-4.307
<b>Metabolism</b>					
CYP2D6 substrate	No	No	No	No	No
CYP3A4 substrate	Yes	Yes	Yes	Yes	No
CYP1A2 inhibitor	Yes	Yes	Yes	Yes	No
CYP2C19 inhibitor	Yes	Yes	Yes	Yes	No
CYP2C9 inhibitor	Yes	Yes	Yes	Yes	No
CYP2D6 inhibitor	No	No	No	No	No
CYP3A4 inhibitor	Yes	Yes	Yes	Yes	No
Total clearance	0.035	0.199	-0.135	-0.045	0.987
<b>Excretion</b>					
Renal OCT2 substrate	No	No	No	No	No
Ames toxicity	Yes	No	Yes	No	No
<b>Toxicity</b>					
Max. tolerated dose (human)	0.895	0.881	0.892	0.887	0.081
hERG I inhibitor	No	No	No	No	No
hERG II inhibitor	Yes	Yes	Yes	Yes	Yes
Oral rat acute toxicity (LD <sub>50</sub> )	2.879	2.902	2.901	2.879	2.408
Oral rat chronic toxicity (LOAEL)	0.014	0.293	0.088	0.14	3.339
Hepatotoxicity	Yes	Yes	Yes	Yes	Yes
Skin sensitization	No	No	No	No	No
<i>Tetrahymena pyriformis</i> toxicity	0.286	0.286	0.286	0.286	0.285
Minnow toxicity	0.392	-0.05	-0.141	-0.801	4.412

Abbreviations: ADMET, absorption, distribution, metabolism, excretion, and toxicity; BBB, blood-brain barrier; CNS, central nervous system; VDss, volume of distribution.

the bioavailability and is significant in determining the dose intervals to achieve the optimum blood level of drug concentrations. Our data demonstrated that compounds **13** and **15**, and doxorubicin reveal the highest total clearance values (0.035, 0.199, and 0.987, respectively) when compared with other ligands, especially **20**, which showed the lowest total clearance value (-0.135). Thus, compounds **13** and **15**,

and doxorubicin could be excreted rapidly, hence requiring shorter dosing intervals to maintain the desired drug concentrations. Unlike doxorubicin, compound **19** showed a slow clearance rate, which means the advantage of longer dosing intervals for the latter. The last parameter analyzed in the pharmacokinetic profile of our newly synthesized triazoles was hepatotoxicity. As shown in Table 3, we can

recognize that all ligands shared the drawback of exhibiting hepatotoxic effects, shown also by the reference drug doxorubicin. Distinguishably, our designed compounds showed extreme better tolerability (0.881–0.895), compared with 0.081 for doxorubicin. Finally, the minimal oral doses needed from the designed compounds for acute rat toxicity (LD<sub>50</sub>) are higher than that of the reference drug.

### 3 | CONCLUSION

In conclusion, we are reporting here the design, synthesis, in vitro anticancer evaluation, SAR, in silico docking, and pharmacokinetic profiling studies of three novel series of 1,2,4-triazole derivatives as potential adenosine A2B receptor antagonists. Our target triazole derivatives were designed on the basis of the structure of previously reported hit compounds as inhibitors of A2B with three main biospecific modifications. Different substitution patterns were introduced at the phenyl groups at both C-5 of the triazole ring and the terminal hydrophilic tail to study the effect of such substituents on the cytotoxicity. Four of our designed derivatives showed good cytotoxicity effects against the human breast adenocarcinoma (MDA-MB-231) cell line as a proven model for A2B adenosine receptor subtype. Compounds **15** showed a more potent inhibitory effect than doxorubicin, with an IC<sub>50</sub> value of 3.48 μM. Also, compound **20** revealed almost an equipotent activity with the reference cytotoxic drug against selected cancer cells, with an IC<sub>50</sub> value of 5.95 μM. In addition, docking study was conducted to evaluate how the most active compounds interacted with the binding pocket of the homology model of A2B receptor. The observed IC<sub>50</sub> values were consistent with the obtained docking scores. Furthermore, SAR analysis and the pharmacokinetic profiling of new compounds were performed. The newly designed compounds revealed prominent pharmacokinetic profiles as compared with the reference marketed drug.

## 4 | EXPERIMENTAL

### 4.1 | Chemistry

#### 4.1.1 | General

Melting points were measured on an electrothermal (Stuart SMP30) apparatus and were uncorrected. IR spectra were recorded on a Pye Unicam SP 1000 IR spectrophotometer at the Pharmaceutical Analytical Unit, Faculty of Pharmacy, Al-Azhar University. <sup>1</sup>H NMR and <sup>13</sup>C NMR spectra were recorded in dimethyl sulfoxide (DMSO)-*d*<sub>6</sub> at 300 and 100 MHz, respectively, on a Varian Mercury VXR-300 NMR spectrometer at NMR Lab, Faculty of Science, Cairo University. Chemical shifts were related to that of the solvent and tetramethylsilane was used as an internal standard. Mass spectra and microanalyses were carried out at the Regional Center for Mycology Biotechnology, Al-Azhar University, Cairo, Egypt. The progress of reactions was monitored with Merck silica gel IB2-F plates (0.25-mm

thickness) and was visualized under a UV lamp, using different solvents as mobile phases. Starting reagents, benzoic acid and acid derivatives, hydrazine hydrate, phenyl isothiocyanate, chloroacetyl chloride, and substituted anilines, were purchased from the Sigma-Aldrich and were used as received. Compounds **11a–c** were synthesized according to directions of reported procedures.<sup>[22,36]</sup>

The original spectra of the investigated compounds are provided as Supporting Information Data. Their InChI codes, together with some biological activity data, are also provided as Supporting Information Data.

#### 4.1.2 | General procedures for the synthesis of *N*-aryl-2-[(4,5-diphenyl-4*H*-1,2,4-triazol-3-yl)thio]-acetamides (**12–21**)

The appropriate 5-(4-substituted-phenyl)-4-phenyl-4*H*-1,2,4-triazole-3-thiol derivatives **11a,b** (0.001 mol) were suspended in a solution of KOH (0.025 mol) in ethanol (30 ml). The appropriate 2-chloro-*N*-arylacetylamide derivative (0.011 mol) was added, and the mixture was heated to 80°C with continuous stirring for 8 hr. After the completion of the reaction (monitored using TLC), the reaction mixture was allowed to stand overnight. The produced solid products were separated by filtration, washed with cold water to remove the inorganic side products, dried, and crystallized from ethanol to obtain the corresponding final compounds (**12–21**).

##### *N*-(4-Bromophenyl)-2-[(4,5-diphenyl-4*H*-1,2,4-triazol-3-yl)thio]-acetamide (**12**)

White solid (0.32 g, 70%); mp: 264–266°C; IR (KBr)  $\nu_{\max}$  cm<sup>-1</sup>: 3,441 (NH), 3,072 (CH aromatic), 2,967 (CH aliphatic), 1,675 (C=O); <sup>1</sup>H NMR (DMSO-*d*<sub>6</sub>)  $\delta$ : 10.21 (brs, 1H, NH), 7.55 (d, *J* = 1.8 Hz, 2H), 7.46 (t, *J* = 1.8 Hz, 1H), 7.40 (d, *J* = 1.8 Hz, 2H), 7.23 (d, *J* = 1.8 Hz, 2H), 7.13 (t, *J* = 1.8 Hz, 2H), 6.89 (d, *J* = 1.8 Hz, 2H), 6.87 (d, *J* = 1.8 Hz, 2H), 4.14 (s, 2H, SCH<sub>2</sub>); <sup>13</sup>C NMR (DMSO-*d*<sub>6</sub>)  $\delta$ : 166.59, (C=O), 154.44, (triazole C-5), 152.78, (triazole C-3), 138.60, (*N*-phenyl C-1), 135.61, (NH-phenyl C-1), 134.46, (phenyl C-4, *N*-phenyl C-4), 131.21, (phenyl C-1), 131.05, (NH-phenyl C-3, C-5), 130.58, (phenyl C-3, C-5), 129.71, (*N*-phenyl C-3, C-5), 128.52, (*N*-phenyl C-4), 128.03, (*N*-phenyl C-2, C-6), 126.36, (NH-phenyl C-2, C-6), 119.60, (phenyl C-2, C-6), 37.70, (SCH<sub>2</sub>); mass spectroscopy (MS; *m/z*, %): 465 (M<sup>+</sup>, 8.15%), 501 (M+2, 2.81%). Anal. calc. for C<sub>22</sub>H<sub>17</sub>BrN<sub>4</sub>OS (M.W. = 465): C, 56.78; H, 3.68; N, 12.04; found: C, 56.80; H, 3.67; N, 12.14%.

##### *N*-(4-Chlorophenyl)-2-[(4,5-diphenyl-4*H*-1,2,4-triazol-3-yl)thio]-acetamide (**13**)

White solid (0.29 g, 70%); mp: 232–234°C; IR (KBr)  $\nu_{\max}$  cm<sup>-1</sup>: 3,416 (NH), 3,062 (CH aromatic), 2,981 (CH aliphatic), 1,682 (C=O), 1,490 (C=C); <sup>1</sup>H NMR (DMSO-*d*<sub>6</sub>)  $\delta$ : 10.2 (brs, 1H, NH), 832 (t, *J* = 1.8 Hz, 1H), 7.60–6.84 (m, *J* = 2.1 Hz, 13H), 3.98 (s, 2H, SCH<sub>2</sub>); <sup>13</sup>C NMR (DMSO-*d*<sub>6</sub>)  $\delta$ : 167.02, (C=O), 153.15, (triazole C-5), 151.91, (triazole C-3), 137.76, (*N*-phenyl C-1), 134.68, (NH-phenyl C-1), 133.53, (phenyl C-4, *N*-phenyl C-4), 130.29, (phenyl C-1), 130.12, (NH-phenyl C-3, C-5), 129.65, (phenyl C-3, C-5), 128.79, (*N*-phenyl C-3, C-5),

127.55, (N-phenyl C-4), 127.11, (N-phenyl C-2, C-6), 125.44, (NH-phenyl C-2, C-6), 120.67, (phenyl C-2, C-6), 36.80, (SCH<sub>2</sub>); MS (*m/z*, %): 420 (M<sup>+</sup>, 24.62%), 422 (M+2, 7.17%). Anal. calc. for C<sub>22</sub>H<sub>17</sub>ClN<sub>4</sub>O<sub>5</sub> (M.W. = 420): C, 62.78; H, 4.07; N, 13.31; found: C, 62.80; H, 4.15; N, 13.50%.

2-[(4,5-Diphenyl-4H-1,2,4-triazol-3-yl)thio]-N-(*p*-tolyl)-acetamide (14)

White solid (0.26 g, 66%); mp: 223–225°C; IR (KBr)  $\nu_{\max}$  cm<sup>-1</sup>: 3,452 (NH), 3,078 (CH aromatic), 2,979 (CH aliphatic), 1,672 (C=O), 1,454 (C=C); <sup>1</sup>H NMR (DMSO-*d*<sub>6</sub>)  $\delta$ : 10.36 (brs, 1H, NH), 7.56–7.35 (m, *J* = 1.8 Hz, 12H), 7.12 (d, *J* = 1.8 Hz, 2H), 4.18 (s, 2H, SCH<sub>2</sub>), 2.49 (s, 3H, CH<sub>3</sub>); <sup>13</sup>C NMR (DMSO-*d*<sub>6</sub>)  $\delta$ : 166.51, (C=O), 154.42, (triazole C-5), 151.67, (triazole C-3), 151.17, (N-phenyl C-1), 148.02, (NH-phenyl C-1), 139.51, (phenyl C-4, N-phenyl C-4), 138.26, (phenyl C-1), 133.82, (NH-phenyl C-3, C-5), 130.02, (phenyl C-3, C-5), 129.94, (N-phenyl C-3, C-5), 129.11, (N-phenyl C-4), 127.77, (N-phenyl C-2, C-6), 127.63, (NH-phenyl C-2, C-6), 123.69, (phenyl C-6), 119.62, (phenyl C-2), 36.74, (SCH<sub>2</sub>), 20.78, (CH<sub>3</sub>), 18.02, (CH<sub>3</sub>); MS (*m/z*, %): 400 (M<sup>+</sup>, 6.15%). Anal. calc. for C<sub>23</sub>H<sub>20</sub>N<sub>4</sub>O<sub>5</sub> (M.W. = 400): C, 68.98; H, 5.03; N, 13.99; found: C, 79.98; H, 5.18; N, 14.16%.

2-[(4,5-Diphenyl-4H-1,2,4-triazol-3-yl)thio]-N-(4-methoxyphenyl)-acetamide (15)

White solid (0.27 g, 66%); mp: 226–228°C; IR (KBr)  $\nu_{\max}$  cm<sup>-1</sup>: 3,422 (NH), 3,072 (CH aromatic), 2,990 (CH aliphatic), 1,672 (C=O), 1,449 (C=C); <sup>1</sup>H NMR (DMSO-*d*<sub>6</sub>)  $\delta$ : 10.19 (brs, 1H, NH), 7.58 (d, *J* = 1.8 Hz, 2H), 7.56 (t, *J* = 1.8 Hz, 1H), 7.46 (d, *J* = 1.8 Hz, 2H), 7.43 (d, *J* = 1.8 Hz, 2H), 7.36 (t, *J* = 1.8 Hz, 2H), 7.34 (d, *J* = 1.8 Hz, 2H), 6.90 (d, *J* = 1.8 Hz, 2H), 4.16 (s, 2H, SCH<sub>2</sub>), 3.72 (s, 3H, OCH<sub>3</sub>); <sup>13</sup>C NMR (DMSO-*d*<sub>6</sub>)  $\delta$ : 164.90, (C=O), 155.36, (triazole C-5), 151.60, (triazole C-3), 133.74, (N-phenyl C-1), 131.91, (NH-phenyl C-1), 130.09, (phenyl C-4, N-phenyl C-4), 129.97, (phenyl C-1), 129.74, (NH-phenyl C-3, C-5), 128.55, (phenyl C-3, C-5), 127.86, (N-phenyl C-3, C-5), 127.61, (N-phenyl C-4), 126.53, (N-phenyl C-2, C-6), 120.64, (NH-phenyl C-2, C-6), 113.90, (phenyl C-2, C-6), 55.14, (OCH<sub>3</sub>), 36.80, (SCH<sub>2</sub>); MS (*m/z*, %): 416 (M<sup>+</sup>, 14.12%). Anal. calc. for C<sub>23</sub>H<sub>20</sub>N<sub>4</sub>O<sub>6</sub>S (M.W. = 416): C, 66.33; H, 4.84; N, 13.45; found: C, 66.38; H, 4.91; N, 13.37%.

2-[(4,5-Diphenyl-4H-1,2,4-triazol-3-yl)thio]-N-(naphthalen-1-yl)-acetamide (16)

White solid (0.31 g, 72%); mp: 222–224°C; IR (KBr)  $\nu_{\max}$  cm<sup>-1</sup>: 3,451 (NH), 3,031 (CH aromatic), 2,924 (CH aliphatic), 1,674 (C=O), 1,553 (C=C); <sup>1</sup>H NMR (DMSO-*d*<sub>6</sub>)  $\delta$ : 10.38 (brs, 1H, NH), 7.68–7.36 (m, 17H), 4.19 (s, 2H, SCH<sub>2</sub>); <sup>13</sup>C NMR (DMSO-*d*<sub>6</sub>)  $\delta$ : 170.20, (C=O), 155.51, (triazole C-5), 149.62, (triazole C-3), 145.34, (N-phenyl C-1), 137.23, (N-phenyl C-1), 134.45, (phenyl C-4), 134.37, (naphthyl C-4a), 131.18, (phenyl C-4), 129.24, (phenyl C-3, C-5), 128.74, (N-phenyl C-3, C-5), 128.55, (N-phenyl C-6), 127.65, (naphthyl C-3), 127.54, (phenyl C-2, C-6), 126.61, (N-phenyl C-2, C-6), 126.10, (naphthyl C-7), 125.70, (naphthyl C-8), 124.64, (naphthyl C-8a), 121.91, (naphthyl C-4), 107.13, (naphthyl C-2), 40.84, (SCH<sub>2</sub>); MS (*m/z*, %): 436 (M<sup>+</sup>,

4.09%). Anal. calc. for C<sub>26</sub>H<sub>20</sub>N<sub>4</sub>O<sub>5</sub> (M.W. = 436): C, 71.54; H, 4.62; N, 12.83; found: C, 71.59; H, 4.70; N, 12.79%.

N-(4-Bromophenyl)-2-[(5-(4-chlorophenyl)-4-phenyl-4H-1,2,4-triazol-3-yl)thio]acetamide (17)

White solid (0.40 g, 84%); mp: 254–256°C; IR (KBr)  $\nu_{\max}$  cm<sup>-1</sup>: 3,438 (NH), 3,052 (CH aromatic), 2,987 (CH aliphatic), 1,675 (C=O), 1,490 (C=C); <sup>1</sup>H NMR (DMSO-*d*<sub>6</sub>)  $\delta$ : 10.47 (brs, 1H, NH), 7.58 (d, *J* = 1.8 Hz, 2H), 7.56 (t, *J* = 1.8 Hz, 1H), 7.53 (d, *J* = 1.8 Hz, 2H), 7.48 (d, *J* = 1.8 Hz, 2H), 7.43 (t, *J* = 1.8 Hz, 2H), 7.41 (d, *J* = 1.8 Hz, 2H), 7.34 (d, *J* = 1.8 Hz, 2H), 4.19 (s, 2H, SCH<sub>2</sub>); <sup>13</sup>C NMR (DMSO-*d*<sub>6</sub>)  $\delta$ : 165.59, (C=O), 153.44, (triazole C-5), 151.78, (triazole C-3), 137.69, (N-phenyl C-1), 134.61, (NH-phenyl C-1), 133.46, (phenyl C-4, N-phenyl C-4), 130.22, (phenyl C-1), 130.05, (NH-phenyl C-3, C-5), 129.58, (phenyl C-3, C-5), 128.71, (N-phenyl C-3, C-5), 127.52, (N-phenyl C-4), 127.03, (N-phenyl C-2, C-6), 125.36, (NH-phenyl C-2, C-6), 120.60, (phenyl C-2, C-6), 36.74, (SCH<sub>2</sub>); MS (*m/z*, %): 499 (M<sup>+</sup>, 04.62%), 501 (M+2, 3.98%). Anal. calc. for C<sub>22</sub>H<sub>16</sub>BrClN<sub>4</sub>O<sub>5</sub> (M.W. = 499): C, 52.87; H, 3.23; N, 11.21; found: C, 52.80; H, 3.36; N, 11.30%.

N-(4-Chlorophenyl)-2-[[5-(4-chlorophenyl)-4-phenyl-4H-1,2,4-triazol-3-yl]thio]acetamide (18)

White solid (0.37 g, 82%); mp: 248–250°C; IR (KBr)  $\nu_{\max}$  cm<sup>-1</sup>: 3,444 (NH), 3,074 (CH aromatic), 2,984 (CH aliphatic), 1,674 (C=O), 1,488 (C=C); <sup>1</sup>H NMR (DMSO-*d*<sub>6</sub>)  $\delta$ : 10.48 (brs, 1H, NH), 7.61 (d, *J* = 1.8 Hz, 2H), 7.58 (t, *J* = 1.8 Hz, 1H), 7.55 (d, *J* = 1.8 Hz, 2H), 7.45 (d, *J* = 1.8 Hz, 2H), 7.43 (t, *J* = 1.8 Hz, 2H), 7.39 (d, *J* = 1.8 Hz, 2H), 7.36 (d, *J* = 1.8 Hz, 2H), 4.20 (s, 2H, SCH<sub>2</sub>); <sup>13</sup>C NMR (DMSO-*d*<sub>6</sub>)  $\delta$ : 165.61, (C=O), 153.46, (triazole C-5), 151.80, (triazole C-3), 137.71, (N-phenyl C-1), 134.63, (NH-phenyl C-1), 133.48, (phenyl C-4, N-phenyl C-4), 130.24, (phenyl C-1), 130.07, (NH-phenyl C-3, C-5), 129.60, (phenyl C-3, C-5), 128.73, (N-phenyl C-3, C-5), 127.54, (N-phenyl C-4), 127.05, (N-phenyl C-2, C-6), 125.38, (NH-phenyl C-2, C-6), 120.62, (phenyl C-2, C-6), 36.76, (SCH<sub>2</sub>); MS (*m/z*, %): 454 (M<sup>+</sup>, 44.97%), 456 (M+2, 14.08%). Anal. calc. for C<sub>22</sub>H<sub>16</sub>Cl<sub>2</sub>N<sub>4</sub>O<sub>5</sub> (M.W. = 454): C, 58.03; H, 3.54; N, 12.30; Found: C, 58.12; H, 3.56; N, 12.36%.

2-[[5-(4-Chlorophenyl)-4-phenyl-4H-1,2,4-triazol-3-yl]thio]-N-(*p*-tolyl)acetamide (19)

White solid (0.29 g, 68%); mp: 235–37°C; IR (KBr)  $\nu_{\max}$  cm<sup>-1</sup>: 3,439 (NH), 3,078 (CH aromatic), 2,979 (CH aliphatic), 1,672 (C=O), 1,507 (C=C); <sup>1</sup>H NMR (DMSO-*d*<sub>6</sub>)  $\delta$ : 10.24 (brs, 1H, NH), 7.57 (d, *J* = 1.8 Hz, 2H), 7.54 (t, *J* = 1.8 Hz, 1H), 7.45 (d, *J* = 1.8 Hz, 2H), 7.42 (d, *J* = 1.8 Hz, 2H), 7.37 (t, *J* = 1.8 Hz, 2H), 7.34 (d, *J* = 1.8 Hz, 2H), 7.10 (d, *J* = 1.8 Hz, 2H), 4.18 (s, 2H, SCH<sub>2</sub>), 2.25 (s, 3H, CH<sub>3</sub>); <sup>13</sup>C NMR (DMSO-*d*<sub>6</sub>)  $\delta$ : 170.23, (C=O), 155.49, (triazole C-5), 149.60, (triazole C-3), 145.33, (N-phenyl C-1), 138.88, (NH-phenyl C-4), 137.57, (NH-phenyl C-1), 136.30, (phenyl C-4), 134.52, (phenyl C-1), 131.36, (phenyl C-3, C-5), 131.26, (NH-phenyl C-3, C-5), 130.95, (phenyl C-2, C-6), 130.70, (N-phenyl C-3, C-5), 130.51, (N-phenyl C-4), 127.61, (N-phenyl C-2, C-6), 123.54, (NH-phenyl C-2, C-6), 38.80, (SCH<sub>2</sub>), 21.33, (CH<sub>3</sub>), 18.02, (CH<sub>3</sub>). Anal. calc. for C<sub>23</sub>H<sub>19</sub>ClN<sub>4</sub>O<sub>5</sub> (M.W. = 434): C, 63.51; H, 4.40; N, 12.88; found: C, 63.60; H, 4.52; N, 13.01%.

*2-[[5-(4-Chlorophenyl)-4-phenyl-4H-1,2,4-triazol-3-yl]thio]-N-(4-methoxyphenyl)acetamide (20)*

White solid (0.34 g, 76%); mp: 238–240°C; IR (KBr)  $\nu_{\max}$   $\text{cm}^{-1}$ : 3,443 (NH), 3,073 (CH aromatic), 2,983 (CH aliphatic), 1,670 (C=O), 1,490 (C=C);  $^1\text{H}$  NMR (DMSO- $d_6$ )  $\delta$ : 10.19 (brs, 1H, NH), 7.58 (d,  $J$  = 1.8 Hz, 2H), 7.45 (t,  $J$  = 3.0 Hz, 1H), 7.34 (d,  $J$  = 3.0 Hz, 2H), 6.90 (d,  $J$  = 3.0 Hz, 2H), 7.43 (t,  $J$  = 6.0 Hz, 2H), 7.39 (d,  $J$  = 1.8 Hz, 2H), 6.90 (d,  $J$  = 1.8 Hz, 2H), 4.17 (s, 2H, SCH<sub>2</sub>), 3.29 (s, 3H, CH<sub>3</sub>);  $^{13}\text{C}$  NMR (DMSO- $d_6$ )  $\delta$ : 161.61, (C=O), 154.46, (triazole C-5), 152.80, (triazole C-3), 138.71, (N-phenyl C-1), 135.63, (NH-phenyl C-1), 134.48, (phenyl C-4, N-phenyl C-4), 131.24, (phenyl C-1), 131.07, (NH-phenyl C-3, C-5), 130.60, (phenyl C-3, C-5), 129.73, (N-phenyl C-3, C-5), 128.54, (N-phenyl C-4), 128.05, (N-phenyl C-2, C-6), 126.38, (NH-phenyl C-2, C-6), 121.62, (phenyl C-2, C-6), 58.70, (OCH<sub>3</sub>), 37.76, (SCH<sub>2</sub>); MS ( $m/z$ , %): 450 (M+, 8.81%), 452 (M+2, 3.01%). Anal. calc. for C<sub>23</sub>H<sub>19</sub>ClN<sub>4</sub>O<sub>2</sub>S (M.W. = 450): C, 61.26; H, 4.25; N, 12.42; found: C, 61.12; H, 4.26; N, 12.39%.

*2-[[5-(4-Chlorophenyl)-4-phenyl-4H-1,2,4-triazol-3-yl]thio]-N-(naphthalen-1-yl)acetamide (21)*

Yellowish white solid (0.31 g, 72%); mp: 253–255°C;  $^1\text{H}$  NMR (DMSO- $d_6$ )  $\delta$ : 10.33 (brs, 1H, NH), 7.56–6.88 (m, 16H), 4.19 (s, 2H, SCH<sub>2</sub>);  $^{13}\text{C}$  NMR (DMSO- $d_6$ )  $\delta$ : 171.23, (C=O), 155.60, (triazole C-5), 150.12, (triazole C-3), 146.31, (N-phenyl C-1), 137.25, (N-phenyl C-1), 134.47, (phenyl C-4), 134.40, (naphthyl C-4a), 131.74, (phenyl C-4), 129.39, (phenyl C-3, C-5), 128.84, (N-phenyl C-3, C-5), 128.65, (N-phenyl C-6), 127.75, (naphthyl C-3), 127.04, (phenyl C-2, C-6), 126.71, (N-phenyl C-2, C-6), 126.10, (naphthyl C-7), 125.34, (naphthyl C-8), 124.80, (naphthyl C-8a), 120.10, (naphthyl C-4), 107.13, (naphthyl C-2), 41.84, (SCH<sub>2</sub>); MS ( $m/z$ , %): 470 (M+, 4.15%), 472 (M+2, 2.83%). Anal. calc. for C<sub>26</sub>H<sub>19</sub>ClN<sub>4</sub>O<sub>2</sub>S (M.W. = 470): C, 66.31; H, 4.07; N, 11.90; found: C, 66.44; H, 4.10; N, 11.99%.

### 4.1.3 | General procedures for the synthesis of 1-aryl-2-[[4-phenyl-5-(p-tolyl)-4H-1,2,4-triazol-3-yl]thio]ethan-1-one derivatives (22, 23)

The mercaptotriazole derivative **11c** (0.27 g, 0.001 mol) was dissolved in a solution of KOH (0.10 g, 0.025 mol) in ethanol (30 ml). The appropriate phenacyl bromide derivative (0.011 mol) was added, and the mixture was stirred at 90°C for 6 hr. After the completion of the reaction (monitored by TLC), the reaction mixture was allowed to stand overnight. The produced precipitates were filtered out, washed with cold water to remove the inorganic side products, dried, and crystallized from ethanol to obtain the corresponding final ketone derivatives (**22**, **23**).

*2-[[4-Phenyl-5-(p-tolyl)-4H-1,2,4-triazol-3-yl]thio]-1-(p-tolyl)ethan-1-one (22)*

White solid (0.33 g, 84%); mp: 237–239°C;  $^1\text{H}$  NMR (DMSO- $d_6$ )  $\delta$ : 7.93–7.35 (m, 9H), 7.22 (d,  $J$  = 8.1 Hz, 2H), 7.14 (d,  $J$  = 8.1 Hz, 2H), 4.88 (s, 2H, SCH<sub>2</sub>), 2.41 (s, 3H, CH<sub>3</sub>), 2.27 (s, 3H, CH<sub>3</sub>);  $^{13}\text{C}$  NMR (DMSO- $d_6$ )  $\delta$ : 211.21, (C=O), 162.61, (triazole C-5), 154.30, (triazole C-3), 151.17,

(N-phenyl C-1), 144.35, (CO-phenyl C-4), 139.52, (CO-phenyl C-1), 133.84, (phenyl C-4), 132.85, (phenyl C-1), 130.81, (phenyl C-3, C-5), 129.92, (CO-phenyl C-3, C-5), 129.17, (CO-phenyl C-2, C-6), 128.51, (N-phenyl C-4), 127.79, (N-phenyl C-3, C-5), 127.60, (phenyl C-2, C-6), 123.79, (phenyl C-4), 36.81, (SCH<sub>2</sub>), 20.86, (CH<sub>3</sub>), 20.79, (CH<sub>3</sub>); MS ( $m/z$ , %): 399 (M+, 23.14%). Anal. calc. for C<sub>24</sub>H<sub>21</sub>N<sub>3</sub>OS (M.W. = 399): C, 72.15; H, 5.30; N, 10.52; found: C, 72.20; H, 5.39; N, 10.54.

*1-(4-Chlorophenyl)-2-[[4-phenyl-5-(p-tolyl)-4H-1,2,4-triazol-3-yl]thio]ethan-1-one (23)*

White solid (0.37 g, 89%); mp: 222–224°C; IR (KBr)  $\nu_{\max}$   $\text{cm}^{-1}$ : 3,045 (CH aromatic), 2,927 (CH aliphatic), 1,674 (C=O), 1,605 (C=C);  $^1\text{H}$  NMR (DMSO- $d_6$ )  $\delta$ : 8.05–7.38 (m, 9H), 7.22 (d,  $J$  = 7.8 Hz, 2H), 7.14 (d,  $J$  = 8.1 Hz, 2H), 4.89 (s, 2H, SCH<sub>2</sub>), 2.26 (s, 3H, CH<sub>3</sub>);  $^{13}\text{C}$  NMR (DMSO- $d_6$ )  $\delta$ : 211.10, (C=O), 162.52, (triazole C-5), 154.36, (triazole C-3), 151.21, (N-phenyl C-1), 144.36, (CO-phenyl C-4), 139.50, (CO-phenyl C-1), 133.82, (phenyl C-4), 132.85, (phenyl C-1), 130.83, (phenyl C-3, C-5), 129.90, (CO-phenyl C-3, C-5), 129.18, (CO-phenyl C-2, C-6), 128.53, (N-phenyl C-4), 127.78, (N-phenyl C-3, C-5), 127.57, (phenyl C-2, C-6), 123.79, (phenyl C-4), 36.82, (SCH<sub>2</sub>), 20.87, (CH<sub>3</sub>); MS ( $m/z$ , %): 419 (M+, 4.39%), 421 (M+2, 1.61%). Anal. calc. for C<sub>23</sub>H<sub>19</sub>ClN<sub>4</sub>O<sub>2</sub>S (M.W. = 454): C, 63.51; H, 4.40; N, 12.88; found: C, 62.51; H, 4.47; N, 13.01%.

## 4.2 | Biological evaluation

### 4.2.1 | In vitro cytotoxic activity

The human breast adenocarcinoma MDA-MB-231 cell line was obtained from VACSERA, Cairo, Egypt, and was allowed to grow in Dulbecco's modified Eagle's medium. MTT assay<sup>[33]</sup> is one of the most widely used tools in cell biology for measuring the metabolic activity, and it was adopted herein to evaluate cytotoxicity. Exponentially growing cells of the MDA-MB-231 cell line were trypsinized, counted, and seeded at the appropriate densities. Cells were then incubated at 37°C for 24 hr in a humidified atmosphere. Next, cells were exposed to five different concentrations of test compounds for 24, 48, and 72 hr. The growth medium was removed; cells were incubated with 200  $\mu\text{l}$  of 5% MTT solution and were allowed to metabolize the dye into a pink-colored insoluble formazan. The remaining MTT solution was discarded from the wells and the produced crystals of formazan were dissolved in 200  $\mu\text{l}$  acidified isopropanol. Absorbance was measured at 570 nm. The cell viability was expressed as a percentage of control, and the concentration that induces 50% of the maximum inhibition of cell proliferation (IC<sub>50</sub>) was determined.

### 4.3 | Docking studies

Molecular docking experiments were performed using the AutoDock Vina program.<sup>[37]</sup> The homology model of A2B receptor and the docking protocol described in an earlier report<sup>[13]</sup> were adapted for this purpose. The identified hit, together with water molecules, was

removed. The protein for docking with AutoDock was prepared using ADT, which includes the addition of polar hydrogens to the protein atoms, followed by assignment of the Kollman charges. For the ligand, all hydrogen atoms were presented to calculate partial atomic charges. A grid was placed over the center of the identified hit to recognize the protein active site. Ligand hydrogens were also added and Gasteiger charges were assigned. All the necessary grid maps were calculated before docking. The grid maps were generated with the help of AutoGrid, which is a program of the AutoDock suite.

## CONFLICTS OF INTERESTS

The authors declare that there are no conflicts of interests.

## ORCID

Hamada S. Abulkhair  <http://orcid.org/0000-0001-6479-4573>

## REFERENCES

- G. Haskó, P. Pacher, E. A. Deitch, E. S. Vizi, *Pharmacol. Ther.* **2007**, *113*, 264. <https://doi.org/10.1016/j.pharmthera.2006.08.003>
- M. Wall, N. Dale, *Curr. Neuropharmacol.* **2008**, *6*, 329. <https://doi.org/10.2174/157015908787386087>
- B. Sperlág, *Handbook of Neurochemistry and Molecular Neurobiology* (Eds: A. Lajtha, E. S. Vizi), Springer, Boston, MA **2008**, pp. 227–254.
- S. Sheth, R. Brito, D. Mukherjee, L. Rybak, V. Ramkumar, *Int. J. Mol. Sci.* **2014**, *15*, 2024. <https://doi.org/10.3390/ijms15022024>
- S. Moro, F. Deflorian, M. Bacilieri, G. Spalluto, *Curr. Pharm. Des.* **2006**, *12*, 2175. <https://doi.org/10.2174/138161206777585265>
- Y. Sun, P. Huang, *Front. Chem.* **2016**, *4*, 37. <https://doi.org/10.3389/fchem.2016.00037>
- M. Panjehpour, M. Castro, K.-N. Klotz, *Br. J. Pharmacol.* **2005**, *145*, 211. <https://doi.org/10.1038/sj.bjp.0706180>
- A. El Maatougui, J. Azaaje, M. González-Gómez, G. Míguez, A. Crespo, C. Carbajales, L. Escalante, X. García-Mera, H. Gutiérrez-de Terán, E. Sotelo, *J. Med. Chem.* **2016**, *59*, 1967. <https://doi.org/10.1021/acs.jmedchem.5b01586>
- I. Feoktistov, A. E. Goldstein, S. Ryzhov, D. Zeng, L. Belardinelli, T. Voyno-Yasenetskaya, I. Biaggioni, *Circ. Res.* **2002**, *90*, 531. <http://www.ncbi.nlm.nih.gov/pubmed/11909816>
- S. Basu, D. A. Barawkar, V. Ramdas, Y. Waman, M. Patel, A. Panmand, S. Kumar, S. Thorat, R. Bonagiri, D. Jadhav, P. Mukhopadhyay, V. Prasad, B. S. Reddy, A. Goswami, S. Chaturvedi, S. Menon, A. Quraishi, I. Ghosh, S. Dusange, S. Paliwal, A. Kulkarni, V. Karande, R. Thakre, G. Bedse, S. Rouduri, J. Gundu, V. P. Palle, A. Chugh, K. A. Mookhtiar, *Eur. J. Med. Chem.* **2017**, *127*, 986. <https://doi.org/10.1016/j.ejmech.2016.11.007>
- Z.-G. Gao, K. A. Jacobson, *Int. J. Mol. Sci.* **2019**, *20*, 5139. <https://doi.org/10.3390/ijms20205139>
- J. Lan, H. Lu, D. Samanta, S. Salman, Y. Lu, G. L. Semenza, *Proc. Natl. Acad. Sci. U. S. A.* **2018**, *115*, 9640. <https://doi.org/10.1073/pnas.1809695115>
- F. Sherbiny, The Human Adenosine A2B Receptor: Homology Modeling, Virtual Screening, and Computer-aided Drug Design, *Dissertation*, Universität Bonn, **2011**. <http://hss.ulb.uni-bonn.de/2011/2422/2422.pdf>
- H. S. Abulkhair, A. Turkey, A. Ghiaty, H. E. A. Ahmed, A. H. Bayoumi, *Bioorg. Chem.* **2020**, *100*, 103899. <https://doi.org/10.1016/j.bioorg.2020.103899>
- A. Turkey, A. H. Bayoumi, A. Ghiaty, A. S. El-Azab, A. A.-M. Abdel-Aziz, H. S. Abulkhair, *Bioorg. Chem.* **2020**, *101*, 104019. <https://doi.org/10.1016/j.bioorg.2020.104019>
- A. Aliabadi, A. Mohammadi-Frarni, M. Azizi, F. Ahmadi, *Pharm. Chem. J.* **2016**, *49*, 694. <https://doi.org/10.1007/s11094-016-1355-8>
- Y.-B. Zhang, W. Liu, Y.-S. Yang, X.-L. Wang, H.-L. Zhu, L.-F. Bai, X.-Y. Qiu, *Med. Chem. Res.* **2013**, *22*, 3193. <https://doi.org/10.1007/s00044-012-0306-5>
- R. Kaur, A. Ranjan Dwivedi, B. Kumar, V. Kumar, *Anticancer Agents. Med. Chem.* **2016**, *16*, 465. <https://doi.org/10.2174/1871520615666150819121106>
- R. Al-Salahi, D. Geffken, M. Koellner, *Chem. Pharm. Bull.* **2011**, *59*, 730. <https://doi.org/10.1248/cpb.59.730>
- J. Carlsson, D. K. Tosh, K. Phan, Z.-G. Gao, K. A. Jacobson, *ACS Med. Chem. Lett.* **2012**, *3*, 715. <https://doi.org/10.1021/ml300097g>
- H. G. Ezzat, A. H. Bayoumi, F. F. Sherbiny, A. M. El-Morsy, A. Ghiaty, M. Alswah, H. S. Abulkhair, *Mol. Divers.* **2020**. <https://doi.org/10.1007/s11030-020-10070-w>
- M. S. R. Murty, K. R. Ram, R. Venkateswara Rao, J. S. Yadav, J. Venkateswara Rao, L. R. Velatooru, *Lett. Drug. Des. Discov.* **2012**, *9*, 276. <https://doi.org/10.2174/157018012799129882>
- A. M. Alafeefy, *J. Saudi Chem. Soc.* **2011**, *15*, 337. <https://doi.org/10.1016/j.jscs.2011.06.019>
- M. T.-N. Alireza Aliabadi, S. Andisheh, Z. Tayarani-Najaran, *Iran. J. Pharm. Res.* **2013**, *12*, 267.
- A. A. Ahmad Mohammadi-Farani, N. Heidarian, *Iran. J. Pharm. Res.* **2014**, *13*, 487.
- M. Botlagunta, B. Kollapalli, L. Kakarla, S. P. Gajarla, S. P. Gade, C. L. Dadi, A. Penumadu, S. Javeed, *Bioinformation* **2016**, *12*, 347. <https://doi.org/10.6026/97320630012347>
- S. Ihmaid, H. E. A. Ahmed, A. Al-Sheikh Ali, Y. E. Sherif, H. M. Tarazi, S. M. Riyadh, M. F. Zayed, H. S. Abulkhair, H. S. Rateb, *Bioorg. Chem.* **2017**, *72*, 234. <https://doi.org/10.1016/j.bioorg.2017.04.014>
- A. M. El-Morsy, M. S. El-Sayed, H. S. Abulkhair, *Open J. Med. Chem.* **2017**, *07*, 1. <https://doi.org/10.4236/ojmc.2017.71001>
- A. A. El-Helby, H. Sakr, I. H. Eissa, H. Abulkhair, A. A. Al-Karmalawy, K. El-Adl, *Arch. Pharm.* **2019**, *352*, e1900113. <https://doi.org/10.1002/ardp.201900113>
- M. H. Hannoun, M. Hagra, A. Kotb, A.-A. M. M. El-Attar, H. S. Abulkhair, *Bioorg. Chem.* **2020**, *94*, 103364. <https://doi.org/10.1016/J.BIOORG.2019.103364>
- A. M. Omar, S. Ihmaid, E.-S. E. Habib, S. S. Althagfan, S. Ahmed, H. S. Abulkhair, H. E. A. Ahmed, *Bioorg. Chem.* **2020**, *99*, 103781. <https://doi.org/10.1016/j.bioorg.2020.103781>
- A.-G. A. El-Helby, R. R. A. Ayyad, M. F. Zayed, H. S. Abulkhair, H. Elkady, K. El-Adl, *Arch. Pharm.* **2019**, *352*, e1800387. <https://doi.org/10.1002/ardp.201800387>
- T. Mosmann, *J. Immunol. Methods* **1983**, *65*, 55.
- D. E. V. Pires, T. L. Blundell, D. B. Ascher, *J. Med. Chem.* **2015**, *58*, 4066. <https://doi.org/10.1021/acs.jmedchem.5b00104>
- A. Beig, R. Agbaria, A. Dahan, *PLOS One* **2013**, *8*, 68237. <https://doi.org/10.1371/journal.pone.0068237>
- A. Turkey, A. H. Bayoumi, F. F. Sherbiny, K. El-Adl, H. S. Abulkhair, *Mol. Divers.* **2020**. <http://dx.doi.org/10.1007/s11030-020-10131-0>
- O. Trott, A. J. Olson, *J. Comput. Chem.* **2010**, *31*, 455. <https://doi.org/10.1002/jcc.21334>

## SUPPORTING INFORMATION

Additional supporting information may be found online in the Supporting Information section.

**How to cite this article:** Turkey A, Sherbiny FF, Bayoumi AH, Ahmed HEA, Abulkhair HS. Novel 1,2,4-triazole derivatives: Design, synthesis, anticancer evaluation, molecular docking, and pharmacokinetic profiling studies. *Arch Pharm.* **2020**;e2000170. <https://doi.org/10.1002/ardp.202000170>